Geomechanics and Engineering, *Vol. 13, No. 3 (2017) 489-504*
DOI: https://doi.org/10.12989/gae.2017.13.3.489

A displacement solution for circular openings in an elastic-brittle-plastic rock

Houxu Huang [*1], Jie Li [1,2], Xiaoli Rong [1], Yiqing Hao [1,3] and Xin Dong [1]

[1] *State Key Laboratory of Disaster Prevention and Mitigation of Explosion and Impact, PLA University of Science and Technology, Nanjing, China*
[2] *School of Mechanical Engineering, Nanjing University of Science and Technology, Nanjing, China*
[3] *High-Tech Institute, Fan Gong-ting South Street on the 12th, Qingzhou, Shandong, China*

(*Received November 02, 2015, Revised March 30, 2017, Accepted April 05, 2017*)

Abstract. The localized shear and the slip lines are easily observed in elastic-brittle-plastic rock. After yielding, the strength of the brittle rock suddenly drops from the peak value to the residual value, and there are slip lines which divide the macro rock into numbers of elements. There are slippages of elements along the slip lines and the displacement field in the plastic region is discontinuous. With some restraints, the discontinuities can be described by the combination of two smooth functions, one is for the meaning of averaging the original function, and the other is for characterizing the breaks of the original function. The slip lines around the circular opening in the plastic region of an isotropic H-B rock which subjected to a hydrostatic in situ stress can be described by the logarithmic spirals. After failure, the deformation mechanism of the plastic region is mainly attributed to the slippage, and a slippage parameter is introduced. A new analytical solution is presented for the plane strain analysis of displacements around circular openings. The displacements obtained by using the new solution are found to be well coincide with the exact solutions from the published sources.

Keywords: brittle plastic rock; H-B strength criterion; slip lines; slippage parameter

1. Introduction

Prediction of the displacement in the rock mass around circular openings at great depth is a common and important problem in mining, tunnels and boreholes. Until now, the mostly widely used models in analyzing the deformation of the rock mass around the circular openings are the elastic-strain-softening model and elastic-brittle-plastic model. Park (2014) derived the similarity solution for a circular opening by employing the elastic-strain-softening model. Alejano *et al*. (2012) used the strain-softening model to study the deformation of the rock mass around the tunnel. Many other researchers also successfully obtained the deformation and mechanical behavior of the rock mass around the circular openings based on the strain-softening model (Zhang *et al*. 2012, Serrano *et al*. 2011). However, compared with the widely use of the strain-softening model in the analysis of the rock masses, the deformation analysis of the circular opening by using the elastic-brittle-plastic model in recent years is rarely. Brown *et al*. (1983) presented closed-form solutions

*Corresponding author, Ph.D. Student, E-mail: wuhanhp14315@163.com

http://www.techno-press.org/?journal=gae&subpage=7 ISSN: 2005-307X (Print), 2092-6219 (Online)

for the displacements of circular openings in elastic-brittle-plastic media. Wang (1996) pointed out the errors in the solutions of Brown *et al*. and presented a numerical solution for the displacement based on the iterative procedure. Carranza and Fairhurst (Carranza 2004, Carranza and Fairhurst 1999) presented a self-similarity solution for the displacement around circular openings in elastic-brittle-plastic rock by using the dimensionless formulation of the H-B criterion. Later, Sharan (2005) pointed out the errors in the solutions by Wang and Brown *et al*. (1983) and presented a simple closed-form solution for the displacement of circular openings in the elastic-brittle-plastic media. Park and Kim (2006) made a concise review on the above works and derived the analytical solutions for a circular opening in elastic-brittle-plastic rock.

However, the solutions of the displacement around the circular openings mentioned above all don't take that the rock masses and the displacement field in the plastic region are discontinuous into consideration. In fact, the mechanism of plastic strain is connected with localized shear and there are slip lines in the plastic region of the rock mass (Kachanov 1971, Revuzhenko and Shemyakin 1977). Besides, the rocks are quasi-brittle materials and the deformation process of rock-like materials is mainly governed by elastic deformation and brittle cracking (Qi *et al*. 2014). Carranza and Fairhurst (1999) pointed out that the insight into the general nature of the solution that can be gained from the classical solution is an important attribute that should not be overlooked. Many practical situations show that compared with the liner M-C yield criterion, the non-liner H-B yield criterion is more appropriate to describe the failure of the rock masses (Hoek and Brown 1980, Sharan 2005, Mohammadi and Tavakoli 2015).

In addition, after yielding there are large numbers of slip lines in the plastic rock, the rock in the plastic region is divided into larger numbers of small elements by the slip lines (Kachanov 1971). The plasticity limit of the elements is higher than that of the macro rock mass, the rock and the displacement fields in the plastic region are discontinuous (Kachanov 1971, Revuzhenko and Shemyakin 1977). In the plastic region, the deformation consists of two parts, the first part is the deformation of the elements, and the second part is caused by the slippages of the elements along the slip lines. Compared with the deformation caused by the slippages, the deformation of the elements is insignificant and can be neglected (Revuzhenko and Shemyakin 1977), i.e., after failure, the deformation of the plastic region is the result of slippages However, this mechanism lacks theoretical study, therefore, obtaining an analytical displacement solution of the rock mass around the circular opening based on this mechanism and the Hoek-Brown criterion seems meaningful and necessary.

This paper deals with an analytical solution of the radial displacement around the circular opening in elastic-brittle-plastic rock mass with slip lines, the rock mass is assumed to obey the H-B yield criterion. Two smooth functions' combination is adopted to describe the discontinuities of the displacement field in the plastic region. A slippage parameter is introduced and a new solution of the displacement, which has direct relations with the slippages of the elements along the slip lines, is presented. In the end, displacements around the circular openings in different cases are calculated by using the presented method.

2. Mathematic description of the discontinuities

When disturbed, there are localized shear and slip lines in the plastic rock, the plastic rock is divided into large numbers of elements by the slip lines, the rock and the displacement field on the shear surfaces are discontinuous (Kachanov 1971, Revuzhenko and Shemyakin 1977).With several restraints, the discontinuous displacement field can be described by the combination of two

smooth functions, $u(r)$ and $A(r)$. The first one is for the meaning of averaging the original displacement field, and the second one is for characterizing the breaks of the original displacement field. Describing the displacement field with this method means together with the smooth (averaged) field of the displacement, the information about the discontinuities, which are lost in the displacement field's averaging process, can also be taken into consideration.

A vector variable in plane problem can be denoted by $r = x_1e_1 + x_2e_2$, and the vector function is $U = U_1e_1 + U_2e_2$ (Huang *et al*. 2003). Assume that: (1) U is smooth enough within the elements (the characteristic sizes of the elements are denoted by l, $l << 1$) and $u(r)$ is an averaged and smooth function for the original displacement field; (2) In the center of the element r_i, there is $u(r_i) = U(r_i)$; (3) The discontinuities of $U(r)$ on the boundaries of two adjacent elements (their centers are in r_i and r_{i+1}, respectively) equal $A(r_i)(r_{i+1} - r_i)$, its degree of accuracy ups to $|r_{i+1} - r_i|^2$; (4) A is a second-order tensor with four smooth components A_{km}, where k, m = 1, 2. Then the original discontinuous displacement field can be described by the combination of a smooth vector field $u(r)$ and a tensor field $A(r)$, of which, the components of tensor A can be expressed as

$$A_{km} = \frac{\partial u_k}{\partial x_m} - \frac{\partial U_k}{\partial x_m} \tag{1}$$

where k, m = 1, 2, assume that during the shear process the density of the rock mass is invariant, and the four components of tensor A are determined only by two invariant functions Γ and Ω

$$A_{11} = \cos 2\theta \cdot \Gamma, \quad A_{22} = -\cos 2\theta \cdot \Gamma, \quad A_{21} = -\Omega + \sin 2\theta \cdot \Gamma, \quad A_{12} = \Omega + \sin 2\theta \cdot \Gamma \tag{2}$$

Eq. (2) shows that the components A_{11} and A_{22}, which normal to the sides of the elements in the non-averaged displacement field are continuous, and Ω can be expressed as

$$\Omega = \frac{1}{2}(A_{12} - A_{21}) = \frac{1}{2}\left(\frac{\partial U_2}{\partial x_1} - \frac{\partial U_1}{\partial x_2}\right) - \frac{1}{2}\left(\frac{\partial u_2}{\partial x_1} - \frac{\partial u_1}{\partial x_2}\right) \tag{3}$$

Let's introduce ω, then Eq. (3) can be expressed as

$$\omega = \Omega + \frac{1}{2}\left(\frac{\partial u_2}{\partial x_1} - \frac{\partial u_1}{\partial x_2}\right) = \frac{1}{2}\left(\frac{\partial U_2}{\partial x_1} - \frac{\partial U_1}{\partial x_2}\right) \tag{4}$$

where U_1 and U_2 are the projections of the original displacement field onto the ox_1 and ox_2 axes; u_1 and u_2 are the projections of the averaged displacement field onto the ox_1 and ox_2 axes; Ω represents the difference of the original curl and the averaged displacement field; ω represents half of the curl of the original displacement field. Since the slip lines in the plastic region around the circular opening are axial symmetry and orthogonal (Kachanov 1971), in order to describe them conveniently, the orthogonal curvilinear coordinates are adopted, and they are defined as

$$\begin{cases} x_1 = x_1(\lambda_1, \lambda_2) \\ x_2 = x_2(\lambda_1, \lambda_2) \end{cases} \tag{5}$$

where λ_1, λ_2 are the basic vectors of the orthogonal curvilinear coordinates. The Cauchy Motion

Law in the orthogonal curvilinear coordinates can be expressed as (Eringen and Suhubi 1975)

$$\sum_{k=1}^{2}\left[\frac{1}{\sqrt{g}}\frac{\partial}{\partial\lambda_k}\left(\sigma_{kl}\frac{\sqrt{g}}{\sqrt{g_{kk}}}\right)+\frac{1}{\sqrt{g_{kk}g_{ll}}}\frac{\partial\sqrt{g_{ll}}}{\partial\lambda_k}\sigma_{kl}-\frac{1}{\sqrt{g_{kk}g_{ll}}}\frac{\partial\sqrt{g_{kk}}}{\partial\lambda_l}\sigma_{kk}\right]+X_{(l)}=0 \tag{6}$$

and the strain tensor in the orthogonal curvilinear coordinates can be expressed as (Eringen and Suhubi 1975)

$$\varepsilon_{kl}=\frac{1}{2}\left[\frac{\sqrt{g_{kk}}}{\sqrt{g_{ll}}}\frac{\partial}{\partial\lambda_l}\left(\frac{u_{(k)}}{\sqrt{g_{kk}}}\right)+\frac{\sqrt{g_{ll}}}{\sqrt{g_{kk}}}\frac{\partial}{\partial\lambda_k}\left(\frac{u_{(l)}}{\sqrt{g_{ll}}}\right)+\frac{\delta_{kl}}{\sqrt{g_{kk}g_{ll}}}\sum_{i=1}^{2}\frac{\partial g_{kk}}{\partial\lambda_l}\frac{u_{(r)}}{\sqrt{g_{rr}}}\right] \tag{7}$$

where $g_k g_l = \delta_{mn}\,(\partial x_m/\partial\lambda_k)(\partial x_n/\partial\lambda_l)$, $g_k g_l = 0$ $(k \neq 1)$, $g_m = (\partial x_k/\partial\lambda_m)i_k$, g is the basic vector of the curvilinear coordinates.

Fig. 1 shows that λ_1 and λ_2 are the basic vector of the curvilinear coordinates, but we can also regard them as two orthogonal slip lines, θ is the included angle between the principal stress and the ox_1 axis, the included angle between the tangent to λ_1 and the ox_1 axis is $\theta - \pi/4$, hence, we can obtain the following expressions (Revuzhenko and Shemyakin 1977)

$$\frac{\partial x_2}{\partial\lambda_1}=\tan\left(\theta-\frac{\pi}{4}\right)\frac{\partial x_1}{\partial\lambda_1},\quad \frac{\partial x_2}{\partial\lambda_2}=\tan\left(\theta+\frac{\pi}{4}\right)\frac{\partial x_1}{\partial\lambda_2},\quad \frac{\partial a_1}{\partial\lambda_2}=-a_2\frac{\partial\theta}{\partial\lambda_1},\quad \frac{\partial a_2}{\partial\lambda_1}=-a_1\frac{\partial\theta}{\partial\lambda_2} \tag{8}$$

where $a_1=\partial l_1/\partial\lambda_1=\sqrt{g_{11}}$, $a_2=\partial l_2/\partial\lambda_2=\sqrt{g_{22}}$ are the Lame constants between the orthogonal curvilinear coordinates and the Cartesian coordinates, l_1 and l_2 are the lengths of the arcs along the corresponding slip lines, λ_1 and λ_2. To describe the slip net, we also need the element dimension. Assume that the two coordinate lines λ_1, λ_2 = const are divided into elemental segments as

$$\Delta\lambda_1=f_1(\lambda_1)\cdot\chi,\qquad \Delta\lambda_2=f_2(\lambda_2)\cdot\chi \tag{9}$$

and the lengths of the element sides at point (λ_1, λ_2) equal

$$l_1=f_1(\lambda_1)\cdot a_1(\lambda_1,\lambda_2)\cdot\chi,\qquad l_2=f_2(\lambda_2)\cdot a_2(\lambda_1,\lambda_2)\cdot\chi \tag{10}$$

The denseness of the slip net is determined by the stress field, but in this paper, we won't

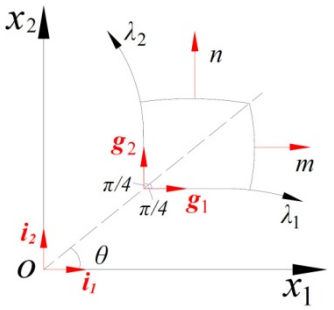

Fig. 1 Cartesian coordinates and Curvilinear coordinates

investigate the development process of the slip lines from regions with higher stresses into regions with lower stresses. In addition, the denseness of the slip net, which is denoted by functions $f_1\chi$ and $f_2\chi$ are assumed to be known. According to Eq. (6), the equilibrium equations in the orthogonal curvilinear coordinates can be expressed as

$$\begin{cases} \dfrac{\partial}{\partial\lambda_1}a_2\sigma_{11}^0+\dfrac{\partial}{\partial\lambda_2}a_1\sigma_{21}^0-a_2\sigma_{12}^0\dfrac{\partial\theta}{\partial\lambda_1}-a_1\sigma_{22}^0\dfrac{\partial\theta}{\partial\lambda_2}+a_1a_2X_1^0=0 \\ \dfrac{\partial}{\partial\lambda_2}a_2\sigma_{12}^0+\dfrac{\partial}{\partial\lambda_2}a_1\sigma_{22}^0+a_2\sigma_{11}^0\dfrac{\partial\theta}{\partial\lambda_1}+a_1\sigma_{21}^0\dfrac{\partial\theta}{\partial\lambda_2}+a_1a_2X_2^0=0 \end{cases} \tag{11}$$

where X_1^0 and X_2^0 are the projections of the body force vectors onto the tangents to the slip lines λ_1 and λ_2; σ_{11}^0, σ_{12}^0, σ_{22}^0 and σ_{21}^0 are the stress components on the slip lines.

The deformation of the media consists of two parts: the deformation within the elements, and the localized shear deformation on the slip lines. As aforementioned, the elastic strains of the elements can be neglected, and in the plane strain problem the deformation normal to the element sides are continuous and can be expressed as (Revuzhenko and Shemyakin 1977)

$$\begin{cases} \varepsilon_{11}^0=\dfrac{1-\nu}{2\mu}\sigma_{11}^0-\dfrac{\nu}{2\mu}\sigma_{22}^0 \\ \varepsilon_{22}^0=\dfrac{1-\nu}{2\mu}\sigma_{22}^0-\dfrac{\nu}{2\mu}\sigma_{11}^0 \end{cases} \tag{12}$$

where ε_{11}^0 and ε_{22}^0 are strains that normal to the element sides. From Eq. (7), the strains can be also expressed as

$$\begin{cases} \varepsilon_{11}^0=\dfrac{\partial u_m}{\partial m}=\dfrac{1}{a_1}\dfrac{\partial w_1}{\partial\lambda_1}-\dfrac{w_2}{a_1}\dfrac{\partial\theta}{\partial\lambda_1} \\ \varepsilon_{22}^0=\dfrac{\partial u_n}{\partial n}=\dfrac{1}{a_2}\dfrac{\partial w_2}{\partial\lambda_2}+\dfrac{w_1}{a_2}\dfrac{\partial\theta}{\partial\lambda_2} \end{cases} \tag{13}$$

In addition, the localized shear strain tangent to the side of the elements can be calculated as

$$\begin{aligned} \frac{\partial u_n}{\partial m}-\frac{\partial U_n}{\partial m}=&\frac{\cos 2\theta}{2}\left(\frac{\partial u_1}{\partial x_1}-\frac{\partial u_2}{\partial x_2}\right)+\frac{\sin 2\theta}{2}\left(\frac{\partial u_2}{\partial x_1}+\frac{\partial u_1}{\partial x_2}\right)+\frac{1}{2}\left(\frac{\partial u_2}{\partial x_1}-\frac{\partial u_1}{\partial x_2}\right) \\ &-\frac{\cos 2\theta}{2}\left(\frac{\partial U_1}{\partial x_1}-\frac{\partial U_2}{\partial x_2}\right)-\frac{\sin 2\theta}{2}\left(\frac{\partial U_1}{\partial x_2}+\frac{\partial U_2}{\partial x_1}\right)-\frac{1}{2}\left(\frac{\partial U_2}{\partial x_1}-\frac{\partial U_1}{\partial x_2}\right) \end{aligned} \tag{14}$$

Generally speaking, for the brittle-plastic rock, $\sigma_{12}^0\neq\sigma_{21}^0$, $\sigma_{12}^0=\tau_+^0+\tau_-^0$, $\sigma_{21}^0=\tau_+^0-\tau_-^0$, ($\tau_+^0$ and τ_-^0 denote two shear stresses systems, the variables with superscript "0" denote the variables on the slip lines). According to the law of symmetry, the elastic shear of the elements only takes place under the effect of the component $\tau_+^0=\left(\sigma_{12}^0+\sigma_{21}^0\right)/2$, and the shear strain can be expressed as

$$\frac{\sigma_{12}^0+\sigma_{21}^0}{4\mu}=\frac{\cos 2\theta}{2}\left(\frac{\partial U_1}{\partial x_1}-\frac{\partial U_2}{\partial x_2}\right)+\frac{\sin 2\theta}{2}\left(\frac{\partial U_1}{\partial x_2}+\frac{\partial U_2}{\partial x_1}\right) \tag{15}$$

According to Eqs. (3), (10) and (14), the slippage on the sides of the elements can be calculated as

$$\begin{cases} \gamma_{12}^0 = \left(\dfrac{\partial u_n}{\partial m} - \dfrac{\partial U_n}{\partial m}\right) l_1 = \left\{\begin{array}{l} \left[\dfrac{\cos 2\theta}{2}\left(\dfrac{\partial u_1}{\partial x_1} - \dfrac{\partial u_2}{\partial x_2}\right) + \dfrac{\sin 2\theta}{2}\left(\dfrac{\partial u_2}{\partial x_1} + \dfrac{\partial u_1}{\partial x_2}\right) - \Omega\right] \\ -\left[\dfrac{\cos 2\theta}{2}\left(\dfrac{\partial U_1}{\partial x_1} - \dfrac{\partial U_2}{\partial x_2}\right) + \dfrac{\sin 2\theta}{2}\left(\dfrac{\partial U_1}{\partial x_2} + \dfrac{\partial U_2}{\partial x_1}\right)\right] \end{array}\right\} f_1 a_1 \chi \\ \gamma_{21}^0 = \left(\dfrac{\partial u_m}{\partial n} - \dfrac{\partial U_m}{\partial n}\right) l_2 = \left\{\begin{array}{l} \left[\dfrac{\cos 2\theta}{2}\left(\dfrac{\partial u_1}{\partial x_1} - \dfrac{\partial u_2}{\partial x_2}\right) + \dfrac{\sin 2\theta}{2}\left(\dfrac{\partial u_2}{\partial x_1} + \dfrac{\partial u_1}{\partial x_2}\right) + \Omega\right] \\ -\left[\dfrac{\cos 2\theta}{2}\left(\dfrac{\partial U_1}{\partial x_1} - \dfrac{\partial U_2}{\partial x_2}\right) + \dfrac{\sin 2\theta}{2}\left(\dfrac{\partial U_1}{\partial x_2} + \dfrac{\partial U_2}{\partial x_1}\right)\right] \end{array}\right\} f_2 a_2 \chi \end{cases} \tag{16}$$

where γ_{12}^0 and γ_{21}^0 are the localized shear on the slip lines; l_1 and l_2 are the lengths of the element sides, which can be also interpreted as inhomogeneous characteristics of the material having the dimension of length. Considering that the shear stresses, which can develop along the slip lines, are determined by the localized shear strain, and then the stress-strain relationship on the slip lines can be expressed as

$$\begin{cases} \gamma_{12}^0 = \gamma\left(\sigma_{12}^0\right) \\ \gamma_{21}^0 = \gamma\left(\sigma_{21}^0\right) \end{cases} \tag{17}$$

Based on Eqs. (12)-(17), on the slip lines the relationship between the stresses and the slippages can be expressed as

$$\begin{cases} \dfrac{\cos 2\theta}{2}\left(\dfrac{\partial u_1}{\partial x_1} - \dfrac{\partial u_2}{\partial x_2}\right) + \dfrac{\sin 2\theta}{2}\left(\dfrac{\partial u_1}{\partial x_2} + \dfrac{\partial u_2}{\partial x_1}\right) - \Omega = \dfrac{1}{f_1 a_1 \chi}\gamma\left(\sigma_{12}^0\right) + \dfrac{\sigma_{12}^0 + \sigma_{21}^0}{4\mu} \\ \dfrac{\cos 2\theta}{2}\left(\dfrac{\partial u_1}{\partial x_1} - \dfrac{\partial u_2}{\partial x_2}\right) + \dfrac{\sin 2\theta}{2}\left(\dfrac{\partial u_1}{\partial x_2} + \dfrac{\partial u_2}{\partial x_1}\right) + \Omega = \dfrac{1}{f_2 a_2 \chi}\gamma\left(\sigma_{21}^0\right) + \dfrac{\sigma_{12}^0 + \sigma_{21}^0}{4\mu} \end{cases} \tag{18}$$

According to Eq. (18), we can obtain the real slippages on the sides of the element, in an elastoplastic body, we can also find that the deformation of the elements is the combination of the stresses σ_{km}^0(i.e., $\sigma_{12}^0, \sigma_{21}^0$) and the moment, the forces between the elements in the plastic region are transmitted via the stresses distributed over their sides.

3. Analysis of the plastic rock with slip lines

Fig. 2 shows that according to the experimental observations (both in the numerical test and the model test), slip lines are easily observed in the elastoplastic material. Assume that the elastic-brittle-plastic rock around the circular opening at great depth is isotropic homogenous, thus, as shown in Figs. 2(c) and (d), after excavation, the slip lines in the plastic rock can be described by the logarithmic spirals (Kachanov 1971).

(a) Numerical result by Andre *et al*. (2014)

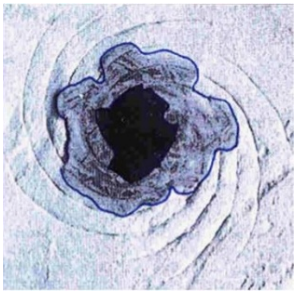

(b) Experimental result by Van den Hoek (2001)

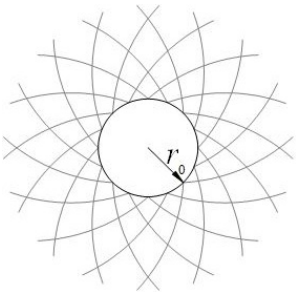

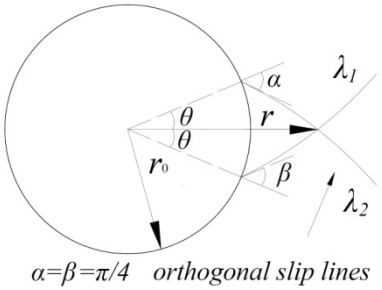

(c) Model of the slip lines around the circular opening (d) Two of the slip lines around the circular opening

Fig. 2 Slip lines around circular opening

$$\begin{cases} \lambda_1 = \dfrac{1}{\sqrt{2}}\left(\ln\dfrac{r}{r_0} - \theta\right) = \text{const} \\ \lambda_2 = \dfrac{1}{\sqrt{2}}\left(\ln\dfrac{r}{r_0} + \theta\right) = \text{const} \end{cases} \tag{19}$$

where λ_1, λ_2 denote the two slip lines, and when the slip lines are logarithmic spirals, it is convenient to describe them with the polar coordinates. The Lame constants between the polar coordinates and the orthogonal curvilinear coordinates are $a_1 = a_2 = r$, and then Eq. (18) can be rewritten as

$$\begin{cases} \dfrac{\partial}{\partial r}(u_r + u_\theta) - \dfrac{1}{r}\dfrac{\partial}{\partial\theta}(u_r + u_\theta) - \dfrac{u_r - u_\theta}{r} - 2\omega = \dfrac{1}{2\mu}(\sigma_r - \sigma_\theta) + \dfrac{2}{f_1 a_1 \chi}\mathrm{S}\left(\dfrac{\sigma_r - \sigma_\theta}{2} - \dfrac{\sigma_{\theta r} - \sigma_{r\theta}}{2}\right) \\ \dfrac{\partial}{\partial r}(u_r - u_\theta) + \dfrac{1}{r}\dfrac{\partial}{\partial\theta}(u_r - u_\theta) - \dfrac{u_r + u_\theta}{r} + 2\omega = \dfrac{1}{2\mu}(\sigma_r - \sigma_\theta) + \dfrac{2}{f_2 a_2 \chi}\mathrm{S}\left(\dfrac{\sigma_r - \sigma_\theta}{2} - \dfrac{\sigma_{\theta r} - \sigma_{r\theta}}{2}\right) \end{cases} \tag{20}$$

where S() represents an operation, considering that the displacements in the surrounding rock are axial symmetry and the dimensions of the elements don't depend on θ, then $f_1(\lambda_1) = f_2(\lambda_2) = 1$, $l_1 = l_2 = \chi r$, in this situation the denseness of the slip lines is described only by χ. Assume that $\sigma_{\theta r} = \sigma_{r\theta} = 0$, $u_\theta = 0$, $X_r = 0$, $X_\theta = 0$, under the axial symmetry condition, we obtain

$$\begin{cases} \dfrac{\partial \sigma_r}{\partial r} + \dfrac{\sigma_r - \sigma_\theta}{r} = 0 \\ \dfrac{\partial u_r}{\partial r} + \dfrac{u_r}{r} = \dfrac{1-2\nu}{2\mu}(\sigma_r + \sigma_\theta) \end{cases} \tag{21}$$

by substituting Eq. (21) into Eq. (20), we have

$$\frac{\partial u_r}{\partial r} - \frac{u_r}{r} = \frac{1}{2\mu}(\sigma_r - \sigma_\theta) + \frac{2}{\chi r}\delta(\tau) \tag{22}$$

where $\tau = (\sigma_\theta - \sigma_r)/2$, $\delta(\tau) = \left(\gamma\left(\sigma_{12}^0\right) + \gamma\left(\sigma_{21}^0\right)\right)/2$.

We can obtain the dimensionless radial displacement from Eqs. (21)-(22) and the displace-ment can be expressed as

$$\begin{cases} \dfrac{u_r}{r} = \dfrac{1-2\nu}{\mu}\displaystyle\int\left(\frac{C_2}{r^3} - \frac{\tau}{r}\right)\mathrm{d}r + C_1 \\ \dfrac{C_2}{r^3} = \dfrac{2\mu}{1-2\nu}\dfrac{\delta(\tau)}{\chi}\dfrac{1}{r^2} + \dfrac{2\tau(1-v)}{1-2\nu}\dfrac{1}{r} \end{cases} \tag{23}$$

where C_1 and C_2 are integration constants which depend on the boundary conditions.

4. Simplified deformation process around circular openings and properties of rock mass

4.1 Simplified deformation process

As shown in the following Fig. 3, the rock mass is assumed to be homogeneous, isotropic, infinitely large and subjected to a hydrostatic in situ stress σ_0. During the excavation process, as the internal pressure p_0 on the opening surface reduced gradually, the radial displacement occurs and a plastic region develops around the opening. After yielding, the strength of the rock suddenly drops from the peak value to the residual value, at the same time the slip lines occurs and the slippages develops rapidly in the plastic region.

Fig. 3 shows the deformation process around the circular opening. At point S_1, the shear stresses in range of $r_0 \le r \le R$ and the displacement on the opening surface both reach their peak values within the rock's elastic stage. From S_1 to S_2, in range of $r_0 \le r \le R$, the strength of the rock mass suddenly drops from its peak value to its residual value, and at the same time, there are slip lines' development and the elements' slippages. In order to simplify the analysis, the slip lines' development and the elements' slippages along the slip lines are assumed to be all completed at point S_2.

The rock mass is divided into numbers of elements by the slip lines, the plasticity limit of the elements separated by the slip lines is much higher than that of the macro rock mass. Compared with the deformation caused by the slippages, the deformation of the elements is insignificant and can be neglected, thus, the deformation takes place between points S_1 and S_2 in range of $r_0 \le r \le R$ should be attributed to the slippages of the elements along the slip lines.

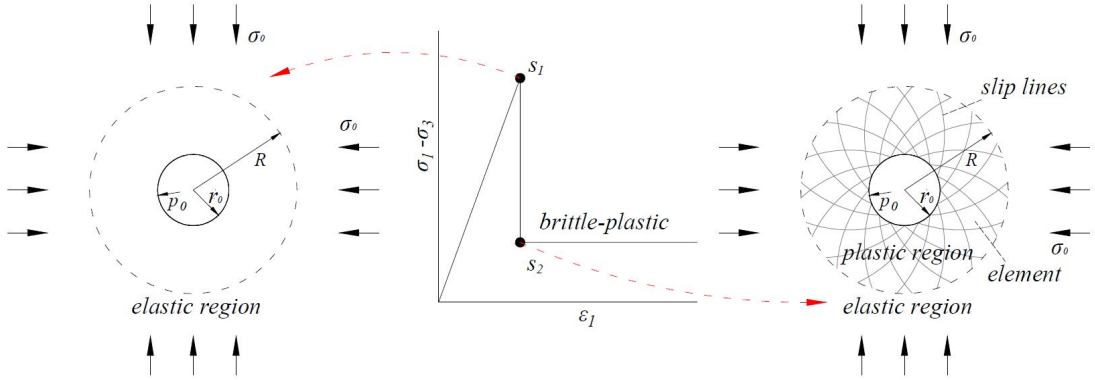

Fig. 3 Slip lines, material behavior and deformation process around circular openings

The analysis also shows that the displacement on the opening surface in elastic-brittle-plastic rock with slip lines can be regarded as the composition of two parts: the first part corresponding to point S_1, in this case: (1) The rock mass and the displacement fields around the circular opening are both continuous; (2) The shear stresses in range of $r_0 \leq r \leq R$ and the displacement on the opening surface both reach their peak values within the elastic stage of the rock. In addition, the other part is caused by the localized shear, i.e., the slippages of the elements along the slip lines. The second part starts from S_1 and ends at point S_2, as shown in Fig. 3. For that the compatibility which is connected with the variability of the curvature of the slip lines will be fulfilled only for sufficiently small strains, thus, the deformation in the surrounding rock with slip lines studied in our paper is also belonging to the small strain problem.

4.2 Material properties

Until now, numbers of criteria such as the revised H-B criterion and those proposed by Xiao *et al*. (2012a) and Yao *et al*. (2004) have been proposed to deal with the rock deformation with considering the effect of the intermediate principal stress. Besides, Xiao *et al*. (2012b) have also proposed a cross-anisotropic criterion to solve the anisotropic rock deformation problem. The aforementioned criteria have provided us with more ways to well deal with the rock deformation problem and we will try to calculate the deformation of surrounding rock by using more criteria in the future. However, for it is our first attempt to calculate the displacement by adopting the slippage mechanism, therefore, in order to simplify the following derivation process, in addition to the aforementioned assumptions, the rock behavior is also assumed to be governed by the H-B criterion given by

$$\sigma_1 = \sigma_3 + \sqrt{m\sigma_c\sigma_3 + s\sigma_c^2} \tag{24}$$

because it is an axial symmetry plane problem, the radial and circumferential stresses are the principal stresses, i.e., $\sigma_r = \sigma_3$, $\sigma_\theta = \sigma_1$, then Eq. (24) can be expressed as

For peak strength

$$\sigma_{\theta 0} = \sigma_{r0} + \sqrt{m\sigma_c\sigma_{r0} + s\sigma_c^2} \tag{25}$$

For residual strength:

$$\sigma_{\theta 1} = \sigma_{r1} + \sqrt{m_r \sigma_c \sigma_{r1} + s_r \sigma_c^2} \tag{26}$$

by substituting Eqs. (25)-(26) into Eq. (21), the expressions of the radial stresses corresponding to the peak strength and residual strength can be respectively expressed as

For peak strength

$$\sigma_{r0} = \frac{m\sigma_c}{4}\left[\ln\left(\frac{r}{r_0}\right)\right]^2 + \left[\ln\left(\frac{r}{r_0}\right)\right]\sqrt{m\sigma_c p_0 + s\sigma_c^2} + p_0 \tag{27}$$

For residual strength

$$\sigma_{r1} = \frac{m_r\sigma_c}{4}\left[\ln\left(\frac{r}{r_0}\right)\right]^2 + \left[\ln\left(\frac{r}{r_0}\right)\right]\sqrt{m_r\sigma_c p_0 + s_r\sigma_c^2} + p_0 \tag{28}$$

the close-form solution for the radius of the elastic-plastic interface can be obtained by considering the continuity of the radial stress at the elastic-plastic interface

$$R = r_0 e^{\left(\frac{F_1 - F_2}{2m_r\sigma_c}\right)} \tag{29}$$

where

$$F_1 = \sqrt{2\sigma_c[8s_r\sigma_c + mm_r\sigma_c + 8m_r\sigma_0 - m_r\sqrt{\sigma_c\left(m^2\sigma_c + 16m\sigma_0 + 16s\sigma_c\right)}]} \tag{30}$$

$$F_2 = \sqrt{16\sigma_c\left(m_r p_0 + s_r\sigma_c\right)} \tag{31}$$

and by substituting Eq. (29) into Eq. (28), the radial stress at the elastic-plastic interface can be obtained as

$$\sigma_R = \frac{m_r\sigma_c}{4}\left[\ln\left(\frac{R}{r_0}\right)\right]^2 + \left[\ln\left(\frac{R}{r_0}\right)\right]\sqrt{m_r\sigma_c p_0 + s_r\sigma_c^2} + p_0 \tag{32}$$

the radial and circumferential stresses in the elastic region are given by Lame solution and can be expressed as

$$\begin{cases} \sigma_{re} = \sigma_0 - \left(\dfrac{R}{r}\right)^2\left(\sigma_0 - \sigma_R\right) \\ \sigma_{\theta e} = \sigma_0 + \left(\dfrac{R}{r}\right)^2\left(\sigma_0 - \sigma_R\right) \end{cases} \tag{33}$$

According to Eqs. (25)-(26) and $\tau = (\sigma_\theta - \sigma_r)/2$, the shear stresses in ranges of $r_0 \le r \le R$ (plastic region) are given by

$$\tau_{p1} = \frac{1}{2}\sqrt{m\sigma_c\sigma_{r0} + s\sigma_c^2} \tag{34}$$

For elastic state in range of $r > R$

$$\tau_e = \left(\frac{R}{r}\right)^2 (\sigma_0 - \sigma_R) \tag{35}$$

According to Eq. (23) and Eqs. (34)-(35), when there is plastic region around the circular opening, the new analytical solution for the dimensionless radial displacement on the opening surface can be expressed as

$$\frac{u_0}{r_0} = 2\frac{\delta(\tau)}{l}\int_{r_0}^{R}\frac{r_0}{r^2}\mathrm{d}r + \frac{1}{\mu}\int_{r_0}^{R}\frac{\tau_{p1}}{r}\mathrm{d}r + \frac{1}{\mu}\int_{R}^{r}\frac{\tau_e}{r}\mathrm{d}r \tag{36}$$

if the rock around the circular opening is elastic, there is no slip line around the circular opening, i.e., $\frac{\delta(\tau)}{l} = 0$, in this situation, the dimensionless radial displacement around the circular opening is

$$\frac{u_0}{r_0} = \frac{1}{\mu}\int_{r_0}^{r}\frac{\tau_e}{r}\mathrm{d}r \tag{37}$$

In this case, the shear stress in range of $r \geq r_0$ can be expressed as $\tau_e = (\sigma_0 - p_0)\frac{r_0^2}{r^2}$, let $r \to \infty$, then Eq. (37) can be rewritten as $\frac{u_0}{r_0} = \frac{1}{\mu}\int_{r_0}^{r}\frac{\tau_e}{r}\mathrm{d}r = \frac{(\sigma_0 - p_0)}{2\mu}$.

In Eq. (36), u_0/r_0 is the dimensionless radial displacement on the opening surface, $2\frac{\delta(\tau)}{l}\int_{r_0}^{R}\frac{r_0}{r^2}\mathrm{d}r$ is the dimensionless radial displacement caused by the slippages of the elements along the slip lines. $\delta(\tau)$ is the slippages on the element sides and it is measurable, l is the length of the element sides. Theoretically, the value of $\delta(\tau)/l$ can be determined by tests and is approximately equal to the axial strain in the uniaxial compression tests corresponding to the situation that the localized shear is completed. $\frac{1}{\mu}\int_{r_0}^{R}\frac{\tau_{p1}}{r}\mathrm{d}r$ denotes the dimensionless radial displacement corresponding to the situation that the shear stresses in range of $r_0 \leq r \leq R$ reach their maximum values. $\frac{1}{\mu}\int_{R}^{r}\frac{\tau_e}{r}\mathrm{d}r$ denotes the dimensionless radial displacement caused by the elastic strain in range of $r > R$.

5. Examples and results

Several example cases are analyzed with the dimensionless displacement expression presented above; displacements computed by using the method in this paper are compared with that obtained by Sharan (2005). Data and properties of the rocks for underground openings are taken from published papers and are presented in Table 1.

Table 1 Properties of rock mass and data for underground openings used for test example cases

No.	Ref.	E (GPa)	v	σ_c	m	s	m_r	s_r	r_0 (m)	σ_0 (MPa)	p_0 (MPa)
1	Carranze *et al*. (1999)	5.5	0.25	30	1.70	0.0039	1.0	0.0	5.0	30.0	5.0
2		60.0	0.20	210	10.84	0.296	1.0	0.01	10.0	100.0	0.0
3	Hoek *et al*. (1998)	90.0	0.20	200	16.0	0.33	1.0	0.01	10.0	90.0	0.0
4		25.0	0.30	150	8.35	0.032	1.0	0.01	Var.	38.0	0.0
5		40.0	0.20	300	7.5	0.1	0.3	0.001	4.0	Var.	0.0
6	Hoek *et al*. (1980)	1.38	0.20	69	0.5	0.001	0.1	0.0	5.33	3.31	Var.
7		27.6	0.20	69	1.5	0.004	Var.	0.0	6.1	20.7	Var.

Table 2 Results obtained by presented method (data in parenthesis are exact solutions by Sharan (2005))

No.	Plastic behavior	R/r_0	$\delta(\tau)/l$	u_0/r_0(%)	Error (%)
1	Brittle plastic	1.885	0.0082	1.439 (1.439)	0
	Brittle plastic	1.885	0.0120	1.796 (1.794)	-0.09
	Brittle plastic	1.885	0.0168	2.247 (2.247)	0
2	Brittle plastic	1.293	0.0011	0.365 (0.368)	0.75
	Brittle plastic	1.293	0.0122	0.868 (0.868)	0
	Brittle plastic	1.293	0.0363	1.960 (1.960)	0
3	Brittle plastic	1.188	0.0004	0.184 (0.184)	0
	Brittle plastic	1.188	0.0090	0.456 (0.454)	-0.35
	Brittle plastic	1.188	0.0278	1.051 (1.051)	0

Table 3 Results obtained by presented method (data in parenthesis are exact solutions by Sharan (2005))

No.	Variable parameter	Value of var. parameter	Plastic behavior	R/r_0	$\delta(\tau)/l$	u_0/r_0 (%)	Error (%)
4	r_0	2.5 (m)	Brittle plastic	1.170	0.0273	1.034 (1.034)	0
		5.0 (m)	Brittle plastic	1.170	0.0273	1.034 (1.034)	0
		10.0 (m)	Brittle plastic	1.170	0.0273	1.034 (1.034)	0
5	σ_0	54 (MPa)	Brittle plastic	1.091	0.0253	0.617 (0.617)	0
		81 (MPa)	Brittle plastic	1.415	0.1368	8.547 (8.544)	-0.03
		108 (MPa)	Brittle plastic	1.747	0.3720	32.769 (32.772)	0.01
6	p_0	0.0	Brittle plastic	1.865	0.0779	7.863 (7.866)	-0.08
		0.055	Brittle plastic	1.560	0.0348	2.975 (2.978)	0.11
		0.172	Brittle plastic	1.360	0.0188	1.382 (1.384)	0.14
7	m_r (p_0 = 5 MPa)	0.3	Brittle plastic	1.201	0.0015	0.132 (0.133)	1.10
		0.08	Brittle plastic	1.425	0.003	0.306 (0.307)	0.41
		0.015	Brittle plastic	2.266	0.0173	2.149 (2.154)	0.22

As shown in Table 1, in order to show the results obtained by using the new analytical solution and the effect of the slippage parameter on the displacement, the ranges of data, which are tested in our paper are wide, where E = 1.3890 GPa, v = 0.2~0.3, σ_c = 30~300 Mpa, m = 0.5~1.6, s = 0.001~0.33, m_r = 0.015~1, s_r = 0~0.01, r_0 = 2.5~10 m, σ_0 = 3.31~108 Mpa, p_0 = 0~5 MPa. Considering that the extent disturbed by the excavation is limited, thus, we only analysis the deformation in range of $r_0 \le r \le 20r_0$.

As shown in Tables 2 and 3, the rock behavior around the circular openings is elastic-brittle-plastic, the slippage parameter, the extent of the plastic region and the displacement on the opening surface are presented in terms of dimensionless forms, $\delta(\tau)/l$, R/r_0 and u_0/r_0, respectively. The errors between the results obtained by using our method and the exact solutions by Sharan (2005) are insignificant.

Besides, the slippage parameter is influenced by so many parameters, such as the opening radius r_0, the in situ stress σ_0, the internal pressure p_0 and the parameter m_r.

Example 1 (or 2, or 3) was analyzed to show that the slippage parameter will have a direct influence on the dimensionless radial displacement. With the other conditions kept invariably, the dimensionless radial displacement will increase with the increasing of the slippage parameter.

Example 4 was analyzed for three different opening radiuses, i.e., r_0 = 2.5, 5.0 and 10.0 m. It shows that with all the other conditions kept invariably, the increasing of the opening radius has no effect on the slippage parameter. For example, the slippage parameter kept invariably and equals 0.0284, although the opening radius increases from 2.5 m to 10.0 m.

Example 5 was analyzed for the in situ stress ranging from σ_0 = 54 Mpa to σ_0 = 108 MPa. It shows that, if the in situ stress is the only variable parameter, then the slippage parameter will increase with the increasing of the in situ stress σ_0. From σ_0 = 54 MPa to σ_0 = 81 MPa, the in situ stress increased by 50%, at the same time, the slippage parameter increased by 462.38%. From σ_0 = 81 MPa to σ_0 = 108 MPa, the in situ stress also increased by 50%, but the slippage parameter only increased by 177.99%. It means if the in situ stress is lower, with the increasing of the in situ stress, there is an obvious increase on the slippage parameter, while the in situ stress reaches a relatively high value, the effect of the in situ stress's increase on the increase of the slippage parameter is limited.

Example 6 was analyzed to show that with other conditions kept invariantly, the increase of the internal pressure p_0 can obviously decrease the slippage parameter. For example, the slippage parameter will decrease from 0.0874 to 0.0197 with the internal pressure increase from 0 to 0.172 MPa.

Example 7 was analyzed for several values of m_r ranging from 0.015 to 0.3. For that the lower the value of m_r, the poorer the residual strength of the rock mass. As m_r decrease from 0.3 to 0.015, the slippage parameter will increase from 0.0016 to 0.0171, i.e., with the other conditions kept invariably, the decrease of m_r will lead to the increase of the slippage parameter.

6. Conclusions

In this paper, the elastic-brittle-plastic model is adopted, and in the plastic region, both the deformations and the discontinuities of the displacement fields are attributed to the slippages of the elements along the slip lines. The discontinuities are described by the combination of two smooth functions, a slippage parameter is introduced to characterize the effect of the slippage on the displacement. A new analytical solution of displacement around the circular openings is presented, and the following conclusions are drawn:

- If there are elastic and plastic regions around the circular opening, the dimensionless radial displacement on the circular opening surface in an isotropic homogeneous rock subjected to a hydrostatic in situ stress can be obtained by using Eq. (36), but if the surrounding rock is elastic, we can obtain the dimensionless radial displacement by using Eq. (37).
- The slippage parameter $\delta(\tau)/l$, whose value is approximately equal to the axial strain in the uniaxial compression tests corresponding to the situation that the localized shear is completed, has direct influences on the deformation of the plastic region, if there is plastic region around the circular opening, the displacement on the opening surface will linearly increase with the increasing of the slippage parameter.
- For rock mass, the slippage parameter is variable, but with other conditions kept invariantly, the slippage parameter will increase with the increasing of the in situ stressv, whereas, it will decrease with the increasing of the internal pressure p_0 and parameter m_r. Generally, the initial stress, the supporting stress and the properties of the rock mass affect the value of $\delta(\tau)/l$ obviously.
- For the elastic-brittle-plastic rock in different cases, the slippage parameter is different; the errors between the displacements obtained by using our method and that by Sharan (2005) are insignificant.
- It is our first attempt to calculate the radial displacement around the circular openings with considering the slippage mechanism, therefore, there are still many issues to be further studied. In our future study, in addition to embedding other criteria into our analysis, we will also try to take the Weibull function distribution of the rock brittleness into consideration, so that to make the solution more in line with the practical engineering.

Acknowledgments

The authors would like to express their sincere gratitude to the financial support by the National Key Basic Research Program of China (Grant No. 2013CB036005), National Natural Science Foundation of China (Grant No. 51527810, 51408607, 51679249); in addition, their appreciation also goes to the editor and the anonymous reviewers for their comments.

References

Alejano, L.R., Dono, R.A. and Veiga, M. (2012), "Platic radii and longitudinal deformation profiles of tunnels excavated in strain-softening rock masses", *Tunn. Undergr. Sp. Technol.*, **30**, 169-182.

Brown, E.T., Bray, J.W. and Ladanyi, B. (1983), "Ground response curves for rock tunnel", *ASCE J. Geotech. Eng.*, **109**(1), 15-39.

Carranze, T.C. (2004), "Elastoplastic solution of tunnel problems using the generalized form of Hoek-Brown failure criterion", *Int. J. Rock. Mech. Min. Sci.*, **41**(3), 629-639.

Carranze, T.C. and Fairhurst, C. (1999), "The elatio-plastic response of underground excavations in rock masses that satisfy the Hoek-Brown failure criteria", *Int. J. Rock. Mech. Min. Sci.*, **36**(6), 777-809.

Eringen, A.C. and Suhubi, E.S. (1975), *Elastodynamics*:*Finite Motions*, Academic Press, New York-London.

Hoek, E. and Brown, E.T. (1980), *Underground Excavations in Rock*, The Institution of Mining and Metallurgy, London, UK.

Hoek, E., Kaiser, P.K. and Bawden, W.F. (1998), *Support of Underground Excavations in Hard Rock*, Balkema, Rotterdam, Netherlands.

Huang, H.X., Fan, P.X., Li, J., Wang, M.Y. and Rong, X.L. (2016), "A theoretical explanation for rock core

disking in triaxial unloading test by considering local tensile stress", *Acta Geophys*., **64**(5), 430-1445.
Huang, K.Z., Xue, M.D. and Lu, W.M. (2003), *Tensor Analysis*, TsingHua Press, Beijing, China.
Jaegar, J.C. and Cook, N.G.W. (1979), *Fundamental of Rock Mechanics*, Champman and Hall, London, UK.
Kachanov, L.M. (1971), *Foundations of the Theory of Plasticity*, Elsevier.
Liu, X.R., Li, D.L., Wang, J.B. and Wang, Z. (2015), "Surrounding rock pressure of shallow-buried bilateral bias tunnels under earthquake", *Geomech. Eng.*, *Int. J.*, **9**(4), 19-37.
Mohammadi, M. and Tavakoli, H. (2015), "Comparing the generalized Hoek-Brown and Mohr-Coulomb failure criteria for stress analysis on the rocks failure plane", *Geomech. Eng.*, *Int. J.*, **9**(1), 115-124.
Müller, A.L., do Amaral Vargas, E. and Gonçalves, C.J. (2014), "Numerical simulation of solids production in slip-lines type breakout modes using standard and Cosserat continua", *J. Petrol. Sci. Eng.*, **122**, 134-148.
Park, K.H. (2014), "Similarity solution for a spherical or circular opening in elastic-strain softening rock mass", *Int. J. Rock. Mech. Min. Sci.*, **71**, 151-159.
Park, K.H. and Kim, Y.J. (2006), "Analytical solution for a circular opening in an elastic-brittle-plastic rock", *Int. J. Rock. Mech. Min. Sci.*, **43**(4), 616-622.
Qi, C.Z., Wang, M.Y., Bai, J.P. and Li, K.R. (2014), "Mechanism underlying dynamic size effect on rock mass strength", *Int. J. Impact Eng.*, **68**, 1-7.
Revuzhenko, A.F. and Shemyakin, E.I. (1977), "Problem of plane strain of hardening and softening plastic materials", *J. Appl. Mech. Tech. Phys.*, **18**(3), 406-420.
Sharan, S.K. (2005), "Exact and approximate solutions for displacements around circular openings in elastic-brittle-plastic Hoek-Brown rock", *Int. J. Rock. Mech. Min. Sci.*, **42**(4), 542-549.
Serrano, A., Olalla, C. and Reig, I. (2011), "Convergence of circular tunnels in elastoplastic rock masses with non-linear failure criteria and non-associated flow laws", *Int. J. Rock. Mech. Min. Sci.*, **48**(6), 878-887.
Van den Hoek, P.J. (2001), "Prediction of different types of cavity failure using bifurcation theory", *Proceedings of the 38th Symposium of the American Rock Mechanics Association*, Washington, D.C., USA, July, pp. 45-52.
Vincenzo, S. and Ghassan, A.S. (2012), "Analytical solution for undrained plane strain expansion of cylindrical cavity in modified cam clay", *Geomech. Eng.*, *Int. J.*, **4**(1), 19-37.
Vu, T.M., Sulem, J., Subrin, D. and Monin, N. (2013), "Semi-analytical solution for stresses and displacements in a tunnel excavated in transversely isotropic formation with non-linear behavior", *Rock Mech. Rock Eng.*, **46**(2), 213-229.
Wang, Y. (1996), "Ground response of circular tunnel in poorly consolidated rock", *ASCE J. Geotech. Eng*, **122**(9), 703-708.
Wang, S.L., Zheng, H., Li, C.G. and Ge, X.R. (2011), "A finite element implementation of strain-softening rock mass", *Int. J. Rock. Mech. Min. Sci.*, **48**(1), 67-76.
Xiao, Y., Liu, H.L., Zhu, J.G. and Shi, W.C. (2012a), "Modeling and behaviours of rockfill materials in three-dimensional stress space", *Sci. China Tech. Sci.*, **55**(10), 2877-2892.
Xiao, Y., Liu, H. and Yang, G. (2012b), "Formulation of cross-anisotropic failure criterion for granular material", *Int. J. Geomech.*, **12**(2), 182-188.
Xiao, Y., Liu, H., Desai, C.S., Sun, Y. and Liu, H. (2016), "Effect of intermediate principal-stress ratio on particle breakage of rockfill material", *J. Geotech. Geoenviron. Eng.*, **142**(4), 06015017.
Yao, Y.P., Lu, D.C., Zhou, A.N. and Zou, B. (2004), "Generalized non-linear strength theory and transformed stress space", *Sci. China Tech. Sci.*, **47**(6), 691-709.
Zhang, Q., Jiang, B.S., Wang, S.L., Ge, X.R. and Zhang H.Q. (2012), "Elasto-plastic analysis of a circular opening in strain-softening rock mass", *Int. J. Rock. Mech. Min. Sci.*, **50**, 38-46.

CC

List of symbols

H-B	Hoek-Brown	$\gamma_{12}^0, \gamma_{21}^0$	localized shear on the slip lines
M-C	Mohr-Coulomb	δ_{mn}	Kronecker delta
$u(r)$	smooth vector field	X	projections of vector of the body force
$A(r)$	smooth tensor field	μ	shear modulus
$U(r)$	vector function	v	Poisson's ratio
Γ	maximum principal shear strain	r_0	opening radius
g	basic vector of the curvilinear coordinates	$f \cdot \chi$	denseness of the slip lines
i_k	basic vector of the Cartesian coordinates	σ_0	in situ stress
e_1, e_2	orthogonal basis	m, s	H-B constants for rock before yielding
σ_r	radial stress	m_r, s_r	H-B constants for rock after yielding
σ_θ	circumferential stress	u_r	radial displacement component
σ_{r0}	radial stress before yielding	u_θ	Circumferential displacement component
$\sigma_{\theta 0}$	circumferential stress before yielding	p_0	internal pressure on the opening surface
σ_{r1}	radial stress after yielding	σ_R	radial stress at elastic-plastic interface
$\sigma_{\theta 1}$	circumferential stress after yielding	R	plastic radius
σ_{re}	radial stress in elastic region	τ_e	shear stress in range of $r > R$
$\sigma_{\theta e}$	circumferential stress in elastic region	l	average length of the element sides
u_0	radial displacement on the opening surface	$\delta(\tau)/l$	dimensionless slippage parameter
σ_c	uniaxial compressive strength of intact rock	$\delta(\tau)$	averaged slippage displacement
a_1, a_2	Lame constants between the polar and the orthogonal curvilinear coordinates	w_1, w_2	projections of the displacement vectors onto the normal to the slip lines λ_1 and λ_2
λ_1, λ_2	basic vector of the orthogonal curvilinear coordinates, or two slip lines	ω	half of the curl of the original displacement field
U_1	projection of the original displacement field onto the ox_1 axis	v	different curl of the original and the averaged displacement fields
U_2	projection of the original displacement field onto the ox_2 axis	τ_{p1}	shear stress before yielding in range of $r_0 \le r \le R$
u_1	projection of the averaged displacement field onto the ox_1 axis	τ_{p2}	shear stress after yielding in range of $r_0 \le r \le R$
u_2	projection of the averaged displacement field onto the ox_2 axis	χ	denseness of the orthogonal slip lines around the circular opening when $f = 1$
U_m	projection of the original displacement vector onto the m direction	u_m	projection of the averaged displacement vector onto the m direction
U_n	projection of the original displacement vector onto the n direction	u_n	projection of the averaged displacement vector onto the n direction